Aust. Met. Mag. 42 (1993) 1-6

Potential predictability of winter rainfall over southern and eastern Australia using Indian Ocean sea-surface temperature anomalies

Wasyl Drosdowsky
Bureau of Meteorology Research Centre, Melbourne, Australia
(Manuscript received May 1992; revised December 1992)

Lagged relationships between winter rainfall over Australia and Indian Ocean sea-surface temperature anomalies are examined. Forecasts of early winter (April to July) rainfall over parts of southern and eastern Australia appear to be feasible from summer to early autumn (December to March) using an index of sea-surface temperature anomalies in an area off the west Australian coast. Similar results are found with the anomalous pressure gradient between the west coast and central Indian Ocean, which serves as an approximation to the meridional component of the geostrophic wind, and suggests that the sea-surface temperature and rainfall anomalies are forced by the anomalous atmospheric circulation.

Introduction

Australia is a predominately dry continent with highly variable rainfall (Nicholls and Wong 1990), and many attempts have been made to forecast these seasonal rainfall fluctuations. Quayle (1929) suggested the use of Darwin pressure anomalies in forecasting rainfall over northern and eastern Australia. This idea was explored further by Priestley (1962, 1963) and verified by Nicholls and Woodcock (1981). Darwin pressure anomalies are one index of the Southern Oscillation (SO). The relationship between rainfall over the entire Australian continent, and a variety of indices of the Southern Oscillation was comprehensively documented by McBride and Nicholls (1983).

The relationship between Australian rainfall and the SO provides the basis for a Seasonal Climate Outlook, issued by the National Climate Centre (NCC) of the Bureau of Meteorology. The major emphases of this service, which uses the Troup (1967) Southern Oscillation Index (SOI), are rainfall forecasts for eastern Australia. The relations with the SO are weak, however, during the late summer and autumn period, when extreme events decay, and over the western third of the continent throughout the year.

More recent research (Nicholls 1989) has suggested a relationship between the first principal component of winter rainfall which covers parts of southern and central Australia and the gradient in sea-surface temperature (SST) between the central Indian Ocean and Indonesia. An important aspect of this relationship is its independence from the SO. This relationship has been explored further (Drosdowsky 1993a,b) using S and T-mode rotated principal component analysis. The sixth T-mode pattern (T6) found by Drosdowsky (1993a), and shown in Fig. 1, closely resembled Nicholls's (1989) first component of winter rainfall anomalies. The positive phase of T6 consists of positive rainfall anomalies extending in a band from the northwest of Western Australia, through central Australia to Tasmania, with a maximum over South Australia. Negative anomalies cover the northeast of the continent.

Corresponding author address: Mr W. Drosdowsky, Bureau of Meteorology Research Centre, GPO Box 1289K, Melbourne, Vic 3001, Australia.

Fig. 1 Location of the 12° latitude by 20° longitude box (solid) over which the COADS SST index and the 15° latitude by 20° longitude box (dashed) over which the MOHSST index are calculated, the stations used for the pressure index and the T6 rainfall pattern.

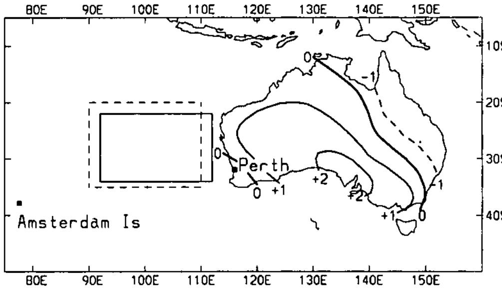

The teleconnection pattern associated with this rainfall pattern (Drosdowsky 1993b) consists of an anomalous low (high) over southern Australia, extending troughs (ridges) northwest into the Indian Ocean and east across the Tasman Sea during wet (dry) winters over southern Australia. This pattern is also related to significant rainfall anomalies over New Zealand, with wet (dry) winters on the east (west) coast occurring during wet winters over southern Australia (Mullan 1991, personal communication).

Nicholls (1989) speculated whether the SST pattern associated with the rainfall anomalies over central and southern Australia was the immediate cause of the rainfall anomalies, or whether both were the result of another unknown forcing. Drosdowsky (1993b) examined this question further using sequences of the composite difference in circulation and SST anomalies between wet and dry winters. Negative SST and positive (southerly) meridional wind anomalies were found in the Indian Ocean as early as March, with anomalies of opposite sign developing north of Australia in the following months. The in-phase development of the SST and the overlying meridional wind anomalies suggests a positive feedback between the SST and atmospheric circulation anomalies, and the possibility, examined in this paper, of using Indian Ocean SST or meridional wind anomalies to forecast winter rainfall over parts of southern and eastern Australia.

Data

The data available in Drosdowsky (1993a) were the monthly totals for the 107 Australian district rainfalls for the period from 1913 through to 1987 as supplied by NCC. The actual data used in the analysis were seasonal anomalies for the period 1950 to 1987. These have been extended through to summer (DJF) 1990–91 for this study. Two predictor indices are developed. The first index consists of area-averaged SST anomalies in the southeast Indian Ocean, while the second index is a pressure difference between Perth on the west Australian coast and Amsterdam Island in the central Indian Ocean. Two versions of the SST index have been calculated, the first using data from the Comprehensive Ocean Atmosphere Data Set (COADS, Slutz et al. 1985) for the period 1950–1986, the second using the United Kingdom Meteorological Office (UKMO) Historical Sea Surface Temperature (MOHSST) data set (Bottomley et al. 1990) for the 1913–1990 period. This data set has been corrected for changes in measurement technique and is considered to be more accurate prior to the 1940s (Allan 1992, personal communication). Data for the stations used in the second index were extracted from the world weather records and NCC. The location of the two SST areas and the stations used in the pressure index are shown in Fig. 1.

Lagged correlations

The large-scale T6 pattern described in Drosdowsky (1993a) and used as initial predictand in this work, had been produced from a reduced set of 62 districts and on seasonal time-scales. Cross-correlations between the winter (JJA) rainfall and autumn (MAM) SST and circulation anomalies (Drosdowsky 1993b) indicated only weak lagged relationships. Similar results have recently been reported by Smith (1993). To assess more precisely the area and time periods, if any, for which useful predictions could be produced, lagged cross-correlations between monthly and bimonthly values of SST anomalies and rainfall were examined.

Firstly correlations were performed between the winter season (JJA) T6 amplitudes and monthly SST anomalies for the period 1950–1986 from COADS over the Indian and west Pacific Oceans. The strongest relationships were found in an area off the west coast of Australia during February (not shown) and March (Fig. 2(b)). The first southeast Indian Ocean index time series was then produced by averaging the anomalies in all available 4° × 4° COADS boxes covering the area 22°S to 34°S and 92°E to 112°E (see Fig. 1). Monthly and bimonthly values of this index were then correlated with the T6 time series and the strong lag relationship confirmed with correlations of −0.41 in February, −0.51 in March and −0.50 in February–March. These correlations are generally greater than the 'simultaneous' values in June (−0.29), July (−0.27) and August (−0.45).

Fig. 2 Pattern of correlations between the time series of the T6 rainfall pattern (Drosdowsky 1993b) and Indian and west Pacific Ocean sea-surface temperatures in (a) January, (b) March, (c) May and (d) July. Contour interval 0.2, with negative contours dashed, and areas significant at the 5 per cent level shaded.

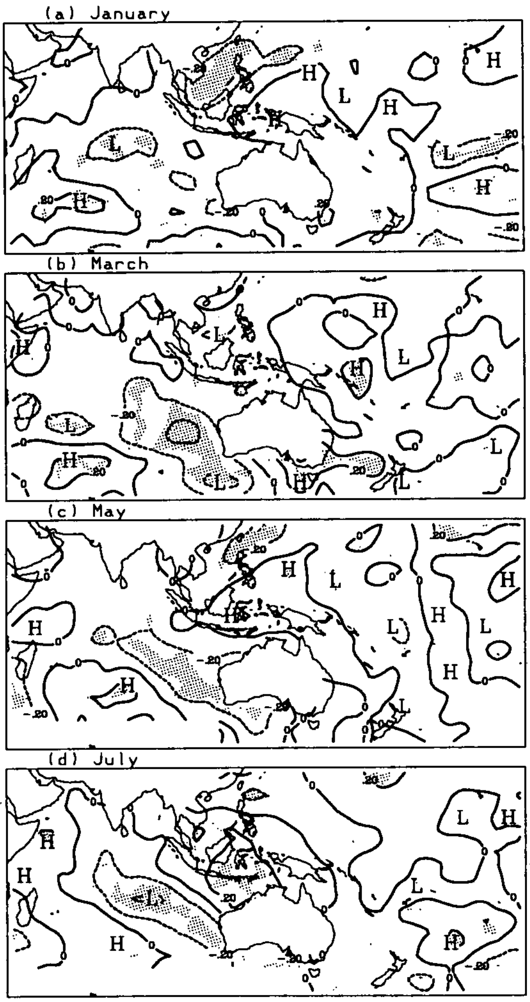

Having identified the late summer/early autumn as the most promising predictor period, overlapping bimonthly values of the COADS SST index from December–January through to April–May were then correlated with similar overlapping bimonthly rainfall totals for all 107 Australian rainfall districts for the periods from April–May through to July–August. This procedure is similar to that used by NCC in utilising the SOI as a predictor of Australian rainfall. The strongest relationships were found with February–March SST correlated with May–June (Fig. 3) and June–July (Fig. 4) rainfall. May–June rainfall over some coastal areas of southern Australia appears to be predictable from the SST index in the previous January–February (Fig. 3(b)). This area expands considerably when February–March SSTs are used (Fig. 3(c)) to cover most of South Australia and extending eastwards into northern Victoria. Significant correlations also develop over southeast Queensland (positive) and the western Top End around Darwin (negative). By March–April (Fig. 3(d)) and April–May (Fig. 3(e)) correlations in the south have diminished in strength and area, while those in the north and on the east coast have strengthened and expanded.

A different pattern is observed with June–July rainfall. Useful correlations are found over parts of southeast Queensland as early as the previous December–January (Fig. 4(a)), while those over southern Australia do not develop until February–March (Fig. 4(c)). These are not as large or extensive as those observed in May–June. While the positive correlations over southeast Queensland are maintained into March–April (Fig. 4(d)) and April–May (Fig. 4(e)), those over northern Australia are not significant. Late winter (July–August) rainfall is not predicted at all by this SST index.

Fig. 3 Lagged correlations between May-June district rainfall and COADS SST index in (a) December-January, (b) January-February, (c) February-March, (d) March-April and (e) April-May.

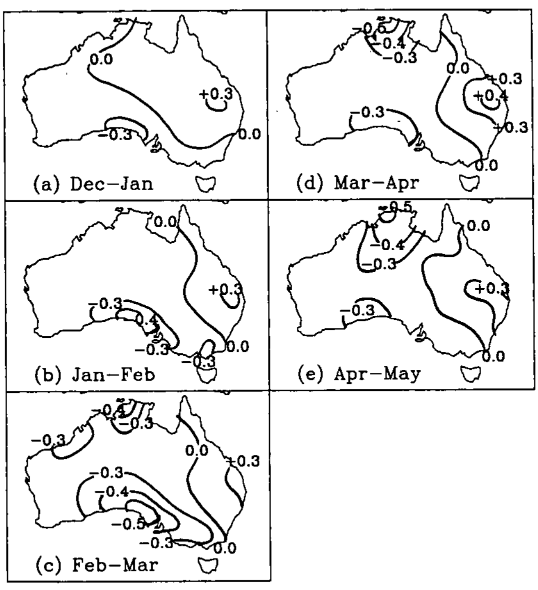

Fig. 4 As for Fig. 3 but for June-July district rainfall.

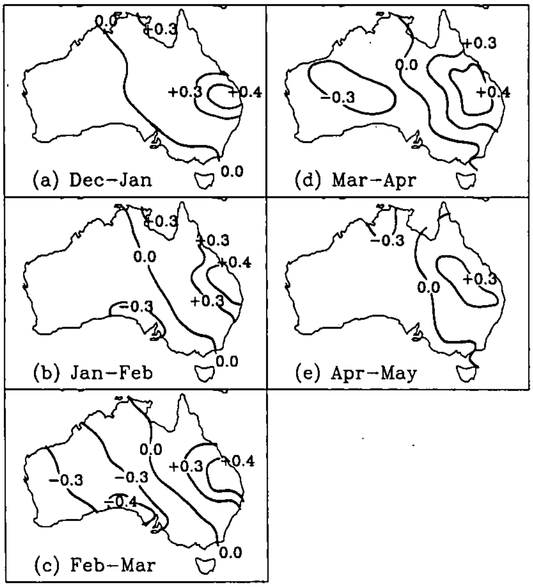

To examine the stability of the relationships, the correlations for May–June rainfall and February–March SST were repeated using the MOHSST data set for 1913–1949 and 1950–1990 and the entire 1913–1990 period. During the later (1950–1990) period the pattern is similar to that shown for the COADS data in Figs 3 and 4. A completely different pattern is found in the earlier period (1913–1949), with generally non-significant positive correlations over most of southern Australia. The pattern of correlations for the entire period is similar to the most recent 1950–1990 period, but with much weaker values. McBride and Nicholls (1983), using data for 1933 to 1974, found similar changes in correlation pattern between Australian rainfall and the SOI when they subdivided their data into two subperiods, 1933–1953 and 1954–1974. They suggest that these changes in the association of Australian rainfall with the SOI may be related to decadal or longer period variability such as documented by Pittock (1975) for mean annual rainfall over southeast Australia, and that better forecasts may be produced by using a shorter, but recent, period of data.

Discussion

Many empirical forecast schemes owe their success to the persistence of the predictor variable, e.g. the SOI. The persistence of the SST index throughout the seasonal cycle is shown in Fig. 5. The most striking features are the very low persistence during the summer months, and the rapid change in late summer/early autumn, when anomalies appear to persist to late winter/early spring. The reasons for this behaviour are not known, but do appear to influence the pattern of lagged correlations between SST and rainfall. If persistence were the sole cause of the forecast skill, then we would expect stronger simultaneous than lagged correlations. In the data examined here the reverse is true, with stronger lagged than simultaneous correlations. This suggests that other factors must also be considered.

As noted earlier, the SST — rain correlation is hypothesised to be due to both being correlated to atmospheric circulation anomalies. In particular wind stress anomalies over the region may precede the SST anomalies and provide even better relationships than those shown in Figs 3 and 4. Rather than derive a wind index similar to the SST index from the COADS, an independent estimate of one component (approximately meridional) of the geostrophic wind over the region was obtained by taking the anomalous pressure gradient between Perth (32°S, 116°E) on the west coast of Australia and Amsterdam Island (38°S, 78°E) in the central Indian Ocean. The index is calculated

Fig. 5 Persistence of monthly values of COADS SST index shown as lagged correlation between base month and following months for up to twelve months ahead. Two annual cycles are shown for clarity. Negative correlations lightly stippled, values greater than 0.4 heavy stipple.

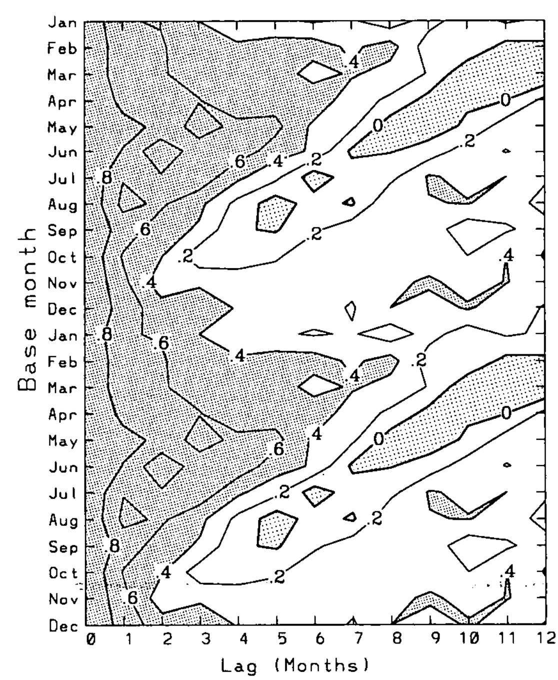

Fig. 6 Lagged cross-correlations between monthly values of COADS SST and pressure difference ('wind') indices (heavy curve), and for individual months December (D), January (J), February (F) and March (M).

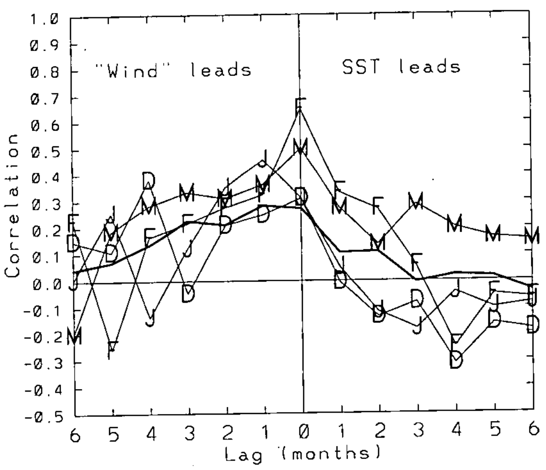

as Amsterdam–Perth pressure anomalies, so that positive (negative) values of the index correspond to southerly (northerly) meridional wind anomalies.

The pressure gradient or 'wind' and SST indices show a markedly asymmetric lagged correlation pattern (Fig. 6), with a tendency for the largest correlations to occur with the SST lagging the pressure gradient (and hence the geostrophic wind) by one month. Figure 6 also shows the lagged correlations for individual months of December through to March. The left (right) half of the figure shows the lagged correlations between the SST ('wind') in the base month (December to March) and the 'wind' (SST) index in the previous one to six months. In December (D) and January (J) the pattern is similar to that for the unstratified time series, with strongest correlations found with 'wind' leading SST. By February (F) and March (M) the simultaneous correlations are much stronger and the pattern more nearly symmetric. Taken together, Figs 5 and 6 suggest some forcing of the SST anomalies by the wind anomalies during summer, with persistence of the SST and 'wind' during autumn and winter then contributing to the rainfall–circulation relationship. The pattern of correlations of the pressure gradient anomalies with the district rainfall (not shown) is similar to those with the SST index, and largest correlations are generally found about one month prior to those observed with the SST index. They exhibit much less spatial or temporal consistency and are less useful for forecasting purposes.

The physical causes of empirical relationships such as those described here can be investigated with general circulation models (GCM). Recently several such modelling experiments have been conducted to investigate the effect of the Indian Ocean SSTs on Australian winter rainfall (Frederiksen et al. 1990; Simmonds 1990; Simmonds and Rocha 1991). These, however, all began with a SST anomaly pattern similar to that observed simultaneously with the rainfall anomalies. The numerical simulation of the empirical results presented here will require the use of coupled ocean–atmosphere models capable of reproducing the observed pattern of persistence in southeast Indian Ocean SST anomalies.

Conclusions

Prediction of early winter (May-June-July) rainfall over parts of southern and eastern Australia is feasible using sea-surface temperatures off the west Australian coast during the previous summer and autumn (December to April) period. The lagged correlations on which this predictability is based are independent of the SO, and in fact extend through the period of weak SOI–rainfall correlations during autumn. These lagged correlations are strongly seasonally and spatially dependent. They are not observed when the usual seasonal groupings (i.e., summer DJF, autumn MAM, and winter JJA) are used, as noted by Drosdowsky (1993b) and Smith (1993). The dipole pattern found in the simultaneous winter correlations is not observed in the lagged correlations, but appears to develop from a small area off the west Australian coast over which the strongest lagged correlations are found. This is again consistent with the results of Smith (1993) who found only weak lagged correlations between the dipole-type pattern in autumn and winter rainfall. The winter dipole does not persist from the previous seasons, but instead evolves steadily during the first half of the year due to forcing by the large-scale atmospheric circulation anomalies.

References

Bottomley, M., Folland, C.K., Hsiung, J., Newell, R.E. and Parker, D.E. 1990. *Global Ocean Surface Temperature Atlas.* United Kingdom Meteorological Office and Massachusetts Institute of Technology, 20 pp. + 313 plates.

Drosdowsky, W. 1993a. An analysis of Australian seasonal rainfall anomalies: 1950–1987. I: Spatial patterns. *Intl J. Climatol.* (in press).

Drosdowsky, W. 1993b. An analysis of Australian seasonal rainfall anomalies: 1950–1987. II: Temporal variability and teleconnection patterns. *Intl J. Climatol.* (in press).

Frederiksen, C.S., Drosdowsky, W., Balgovind, R.C. and Nicholls, N. 1990. 'Indian Ocean sea surface temperatures and Australian rainfall'. *Proceedings, International TOGA Scientific Conference*, WCRP-43, 229–39.

McBride, J.L. and Nicholls, N. 1983. Seasonal relationships between Australian rainfall and the Southern Oscillation. *Mon. Weath. Rev., 111*, 1998–2004.

Nicholls, N. 1989. Sea surface temperatures and Australian winter rainfall. *Jnl climate, 2*, 965–73.

Nicholls, N. and Woodcock, F. 1981. Verification of an empirical long-range weather forecasting technique. *Q. Jl R. met. Soc., 107*, 973–6.

Nicholls, N. and Wong, K. 1990. Dependence of rainfall variability on mean rainfall, latitude and the Southern Oscillation. *Jnl climate, 3*, 163–70.

Pittock, A.B. 1975. Climatic change and the patterns of variation in Australian rainfall. *Search, 6*, 498–504.

Priestley, C.H.B. 1962. Some lag associations in Darwin pressure and rainfall. *Aust. Met. Mag. No. 38*, 32–42.

Priestley, C.H.B. 1963. Some associations in Australian monthly rainfalls. *Aust. Met. Mag. No. 41*, 12–21.

Quayle, E.T. 1929. Long range rainfall forecasting from tropical (Darwin) air pressures. *Proc. R. Soc. Victoria, 41*, 160–4.

Simmonds, I. 1990. A modelling study of winter circulation and precipitation anomalies associated with Australian region ocean temperatures. *Aust. Met. Mag., 38*, 151–62.

Simmonds, I. and Rocha, A. 1991. The association of Australian winter climate with ocean temperatures to the west. *Jnl climate, 4*, 1147–61.

Slutz, R.J., Lubker, S.J., Hiscox, J.D., Woodruff, S.D., Jenne, R.L., Joseph, D.H., Steurer, P.M. and Elms, J.D. 1985. *Comprehensive Ocean Atmosphere Data Set; Release 1*. NOAA Environmental Research Laboratories, Climate Research Program, Boulder, CO. 268 pp. (NTIS PB86-105723).

Smith, I.N. 1993. The potential for improved predictability of Australian seasonal rainfall using sea surface temperatures. *Intl J. Climatol.* (accepted).

Troup, A.J. 1967. Opposition of anomalies in upper tropospheric winds at Singapore and Canton. *Aust. Met. Mag., 15*, 32–7.